Monthly Notices
of the
ROYAL ASTRONOMICAL SOCIETY

MNRAS **469,** S723–S730 (2017)
Advance Access publication 2017 October 13

doi:10.1093/mnras/stx2628

Modelling the size of the very dynamic diamagnetic cavity of comet 67P/Churyumov–Gerasimenko

Aniko Timar,[1,2] Z. Nemeth,[1⋆] K. Szego,[1] M. Dosa,[1] A. Opitz,[1] H. Madanian,[3] C. Goetz[4] and I. Richter[4]

[1] *Wigner Research Centre for Physics, Konkoly-Thege M. Rd. 29-33, H-1525 Budapest, P.O.B. 49, Hungary*
[2] *Eötvös Loránd University, H-1053 Egyetem tér 1-3, Budapest, Hungary*
[3] *University of Kansas, 1450 Jayhawk Blvd. Lawrence, KS 66045, USA*
[4] *Institut für Geophysik und extraterrestrische Physik, TU Braunschweig, Mendelssohnstr. 3, D-38106 Braunschweig, Germany*

Accepted 2017 October 6. Received 2017 August 2; in original form 2017 March 31

ABSTRACT

After the first detection of the diamagnetic cavity of comet 67P/Churyumov–Gerasimenko, it became apparent that the boundary of this plasma region is very dynamic. To date hundreds of short cavity crossing events were detected, none lasting longer than an hour. This intermittent set of short events is very different from the classical cavity observation near 1P/Halley, where *Giotto* remained continuously inside the cavity. The distance of the cavity boundary at 67P is larger than that predicted by recent models, so it was not clear whether these short cavity-like regions are connected to a global diamagnetic cavity, or they are due to some local effects. Here, we revisit the neutral-drag model of Cravens (1986) and we provide a very good phenomenological approximation for the highly variable size of this dynamic region. The model uses the cometary neutral production rate and the solar wind dynamic pressure as inputs. For the production rate, we use averaged and detrended data derived from *Rosetta* Orbiter Spectrometer for Ion and Neutral Analysis neutral density measurements. We show that instead of the local neutral pressure, the global production rate drives the size of the cavity. The solar wind pressure is derived from space weather models and independently from the magnetic field measurements of Rosetta Magnetometer (MAG). We accurately estimate the highly variable size of the cavity using this data. Our results suggest that at the time of the measurements a global diamagnetic cavity existed around comet 67P, the size of which varied dynamically following the changing cometary gas production and solar wind pressure.

Key words: magnetic fields – plasmas – methods: data analysis – comets: individual: 67P/Chuyumov–Gerasimenko.

1 INTRODUCTION

Comets are among the oldest objects in the Solar system, characterized by their highly elliptical orbit and bright atmosphere composed of dust and volatiles (Balsiger et al. 2007; Gombosi 2015; Nilsson et al. 2015a). Nearing perihelion, the neutral coma expands and is continuously ionized. The two main ionization mechanisms are photoionization by the incident ultraviolet radiation of the Sun (Mendis, Houpis & Marconi 1985; Cravens 1991; Vigren et al. 2015; Madanian et al. 2016a) and impact with high-energy electrons (Gan & Cravens 1990; Galand et al. 2016). Due to the continuous gas outflow from the nucleus and the ionization of the neutral species, the cometary magnetosphere significantly differs from the magnetosphere of other non-magnetic Solar system bodies (Russell et al. 1982). The *Rosetta* mission (Glassmeier et al. 2007b) presents an excellent opportunity to discover the nature of the cometary magnetospheres and learn about the various structures created by the interaction between the solar wind and the cometary atmosphere (Cravens 1989a).

In this paper, we approximate the extent of one of these structures, the diamagnetic cavity around comet 67P/Churyumov–Gerasimenko (67P), based on the measurements of the *Rosetta* spacecraft and various solar wind models using the neutral-drag model of Cravens (1986). Approaching the comet, the solar wind slows down which sometimes also gives rise to a bow shock (Biermann, Brosowski & Schmidt 1967; Galeev, Cravens & Gombosi 1985; Szegö et al. 2000; Koenders et al. 2013). Using a quasi-hydrodynamical approach, Biermann et al. (1967) demonstrated that around a comet with sufficiently high outgassing rate, the solar wind is slowed down and redirected at the cometary contact surface, a boundary region that separates the solar wind and the

⋆E-mail: nemeth.zoltan@wigner.mta.hu

plasma of purely cometary origin. Taking the magnetic field into consideration and assuming the field lines are frozen into the plasma flow, the magnetic field magnitude and plasma density increase as the flow decelerates: the magnetic field 'piles-up', before reaching the contact surface. Here, the pile-up stops and (if the comet itself is non-magnetic) the field magnitude drops to zero since the solar wind is unable to enter through the boundary. One can say that the resulting magnetic field free region around the nucleus is the diamagnetic cavity. This simplistic picture is however misleading, as the frozen-in field property only guarantees that the plasma content of a flux tube remains on the same flux tube during the evolution of the system, but it does not constrain the plasma density distribution along the tube. It is possible that some parts of the flux tube are 'empty' although the magnetic field is still present. Let us consider a non-magnetic, non-conducting body in the solar wind: the plasma cannot penetrate this body, but the magnetic field lines carried by the plasma are able to do so. Similarly, in the case of a comet, the magnetic field will only be absent if there is a mechanism actively expelling it from the vicinity of the nucleus, and an appropriate description of this phenomenon should contain such a mechanism. This property of the cometary magnetosphere was amply demonstrated by the *Rosetta* Rosetta Plasma Consortium (RPC) experiment, which observed the disappearance of the solar wind (Nilsson et al. 2015b; Behar et al. 2016) in the spring of 2015, but no significant change in the magnetic field accompanied this plasma boundary.

The diamagnetic cavity was first discovered by the *Giotto* spacecraft, which encountered comet 1P/Halley on 1986 March 14 (Neubauer et al. 1986; Reinhard 1986). At a distance of 4760 km from the comet, after passing through a narrow boundary layer, where the magnetic field magnitude dropped abruptly from 20 nT to almost zero, the spacecraft entered the field-free region. Here, the magnetic field stayed continuously near zero for 8513 ± 7 km (Neubauer et al. 1986). These observations helped to identify the mechanism, which keeps the magnetic field away from the vicinity of the active nucleus. Cravens (1986) and Ip & Axford (1987) came to the conclusion that at the diamagnetic cavity boundary the magnetic pressure and magnetic tension built up by the incoming solar wind are balanced out by the ion–neutral friction force inside the cavity boundary, thus defining the extent of the field-free region:

$$\nabla \frac{B^2}{2\mu_0} - \left(\frac{B}{\mu_0}\nabla\right) B = m_\mathrm{i} n_\mathrm{i} \nu_\mathrm{in} (u_\mathrm{n} - u_\mathrm{i}) \quad (1)$$

where B is the magnetic field, n_i, m_i and u_i are the number density, mass and velocity of cometary ions, u_n is the neutral velocity and ν_in is the ion–neutral collision coefficient. The first term on the left-hand side is the magnetic pressure gradient, the second term is the magnetic tension and the right-hand side is the ion–neutral friction force. At the diamagnetic cavity boundary, the velocity of the ions can be neglected as they come to a halt arriving to the boundary (Balsiger et al. 1986). If the curvature radius of the field lines is large, the magnetic tension is also negligible compared to the magnetic pressure.

The *Rosetta* spacecraft arrived at comet 67P/Churyumov–Gerasimenko in 2014 August, providing a unique opportunity to study the comets plasma environment and among others the evolution of the diamagnetic cavity as the comet approaches and eventually passes perihelion. The cavity was first detected by the *Rosetta* 'RPC-Rosetta Magnetometer (MAG)' magnetometer in 2015 July (Goetz et al. 2016a), at a distance of almost 1.24 AU from the Sun, a few weeks before the comet reached its perihelion. Based on this detection, Goetz et al. (2016a,b) reported that the distance of the diamagnetic cavity boundary from the nucleus is larger than expected by recent models (Rubin et al. 2012; Koenders et al. 2015; Huang et al. 2016), and speculated that the detection of the cavity was possible due to the propagation of plasma instabilities along the global cavity boundary, which increased the local extent of the cavity.

Detailed analysis of charged particle and magnetic measurements performed by the RPC revealed that the spacecraft dived into the diamagnetic cavity of comet 67P/Churyumov–Gerasimenko hundreds of times in the course of 10 months (Goetz et al. 2016b; Nemeth et al. 2016). Most of the cavity crossings were only 1–2 min long, and the longest lasted for only 40 min. This is very different from the classical cavity encounter at Halley, where the spacecraft travelled much more distance inside the field-free region (Cravens 1986; Neubauer et al. 1986); however, *Giotto* and *Rosetta* trajectories are also fundamentally different. While *Giotto* performed a rapid flyby, *Rosetta* escorts the comet moving very slowly with respect to the nucleus. A possible explanation for the intermittent cavity crossings at 67P is that the *Rosetta* spacecraft is orbiting very close to the boundary of the diamagnetic cavity of comet 67P, and the fast variations in the force balance between the magnetic field and the outgassing rate are causing the cavity boundary to travel through the spacecraft, allowing *Rosetta* to rapidly enter and exit the diamagnetic cavity. In the case of comet 1P/Halley, *Giotto*'s velocity may had been too high and/or it had travelled too deep inside the cavity to perceive this dynamics. Perhaps there are Kelvin–Helmholtz or Rayleigh–Taylor instabilities propagating along the cavity boundary (Ershkovich & Mendis 1986; Ershkovich & Flammer 1988; Goetz et al. 2016a) of comet 67P that can create short, intermittent cavity crossing events as the spacecraft travels through these instabilities. It is also possible that the cavity boundary is more dynamic at comet 67P than at 1P/Halley. Here, we argue that the first possibility (variations in the force balance between the magnetic field and the outgassing rate) provides a simple and accurate explanation for the dynamics.

Since its first detection at 67P, the nature of the diamagnetic cavity has been investigated in several papers. Goetz et al. (2016b) examined the distribution and shape of the cavity crossing events, and found two type of cavity events, single and clustered, and also reported that the boundary distance does not depend on short-time outgassing rate variations nor on the rotational rate of the comet. They also found that when entering and exiting the cavity, the inbound pass is in average almost three times longer than the outbound pass. Eriksson et al. (2016) showed that the appearance of cold plasma (<0.1 eV) is more frequent while cavity events are present. Distinct cavity signatures were identified by Nemeth et al. (2016) in the thermal and suprathermal electron populations and in the ion spectra. They speculated that the suprathermal electron population is bound to the magnetic field lines, thus expelled from the diamagnetic cavity, causing characteristic drop-outs in the electron spectrum inside the field-free zone, and attributed the detection of ion bursts near the edge of the cavity to strongly negative values of the spacecraft potential caused by the increased density of thermal plasma in the boundary (Cravens 1989b; Goldstein et al. 1989; Odelstad et al. 2015). A detailed study by Madanian et al. (2016b) also reported lower suprathermal electron fluxes inside the diamagnetic cavity. Henri et al. (2017) investigated the properties of the thermal plasma in and near the cavity. They found that the variation of the plasma density inside the cavity events closely follows the smooth variation of the neutral density, while there are strong fluctuations outside; the radial density profile of the unmagnetized plasma decreases as $1/r$.

In this work, we use *Rosetta* magnetic field and neutral density measurements of the RPC-MAG (Glassmeier et al. 2007a) and *Rosetta* Orbiter Spectrometer for Ion and Neutral Analysis (ROSINA; Balsiger et al. 2007) instruments, together with the data of various solar wind models to calculate the extent of this very dynamic diamagnetic cavity. We show that the boundary distance calculated by the neutral-drag model of Cravens (1986) is in a very good agreement with the cavity observations at comet 67P. Modelling the evolution of the boundary distance also helps us to understand what defines the extent of the cavity and what the driving force is behind its dynamics.

2 DATA AND METHOD

According to the neutral-drag model of Cravens (1986), the diamagnetic cavity boundary distance (r_{rcs}) can be calculated as

$$r_{cs} = c\frac{Q^{3/4}}{B_0}, \tag{2}$$

where c is constant, $c = 7.08 \times 10^{-18}$ kmnTs$^{3/4}$, B_0 [nT] is the maximum of the magnetic field in the pile-up region and Q [molecule s^{-1}] is the neutral production (outgassing) rate. Nemeth et al. (2016) reported that a $r_{cs} \sim Q^{3/4}$ agrees well with the average positions of *Rosetta* cavity observations, but with some notable unexplained exceptions and short-scale dynamics. Equation (2) goes one step further, and takes into account the effect of the magnetic field variations as well. B_0 is essentially a measure of the solar wind dynamic pressure (p_{sw}), as the magnetic pressure of the draping region balances the dynamic pressure of the incoming solar wind. Due to its interaction with the cometary plasma, the incoming solar wind slows down, thus forming the cometary induced magnetosphere. As a result, the energy represented by the dynamic pressure of the undisturbed solar wind transfers into the enhanced magnetic field of the draping region. On the outside of this region, the resulting high magnetic pressure balances with the pressure of the incoming solar wind $p_{sw} \sim B_0^2$, while on its inner boundary (which is the cavity boundary) the magnetic pressure is balanced by the neutral drag. Thus,

$$r_{cs} = c\frac{Q^{3/4}}{\sqrt{2\mu_0 p_{sw}}}. \tag{3}$$

The ROSINA Comet Pressure Sensor (COPS) in situ measurements (Balsiger et al. 2007) provide the local neutral density around the comet. Hansen et al. (2016) calculated the total water production rates from the neutral density measurements of ROSINA DFMS and COPS. They used an empirical coma model to correct for the spacecraft motion, the radial distance from the comet, and the Sun-fixed longitude and latitude, then averaged over a cometary rotation period.

The outer driving force on the diamagnetic cavity is the solar wind dynamic pressure. During the observations of the inner region of the cometary magnetosphere by the *Rosetta* orbiter, there were no simultaneous solar wind measurements in front of the comet, hence we tested several independent methods to estimate the solar wind dynamic pressure. Various space weather models can be used to propagate solar wind parameters measured elsewhere to the position of comet 67P. Additionally, it is usually possible to estimate the solar wind dynamic pressure from the maximum of the magnetic field magnitude in the pile-up region. Unfortunately, there are no direct measurements for that quantity either, but it can be estimated from local magnetic field measurements. We will show two such estimation schemes in Section 2.

We use three different category of methods to calculate the boundary distance, one using the solar wind dynamic pressure data from various solar wind models, and two using the local *Rosetta* magnetic field measurements to estimate B_0 in two different ways.

Our first method uses equation (3) to calculate the boundary distance. We obtained the solar wind velocity v and density ρ measurements from various solar wind models and calculated the solar wind dynamic pressure as $p_{sw} = \frac{1}{2}\rho v^2$. During the investigated time period, the solar source was changing and there were several transient events throughout the heliosphere making it difficult to estimate the background solar wind arriving at the comet. Moreover, all solar probes were far from the comet considering heliocentric longitudes (>60 deg), which makes the prediction reliability lower due to the temporal evolution of the solar source. Our space weather model had to handle all these difficulties, which we solved by comparing several different predictions and characterizing the reasons for differences. We compared the results of three different propagation methods:

(1) The simple ballistic model extrapolates solar wind observations to the comet assuming that the solar wind bulk velocity does not change during radial propagation (equations can be found in Opitz et al. 2009 and Vennerstrom et al. 2003).
(2) The 'magnetic lasso' model is an enhanced ballistic method based on the reconstruction of the magnetic connectivity between the solar source and the target (Dósa & Opitz 2017).
(3) The mSWiM model by Zieger & Hansen (2008) applies 1D MHD method for the radial propagation and ballistic propagation to account for the solar rotation.

These methods perform best for quiet solar wind and CIRs, while CMEs represent datagaps due to different propagation properties. The first two were applied both to the OMNI solar wind data measured in the vicinity of the Earth and to the data measured by the *STEREO-A* spacecraft, which was in opposition to the Earth at the time of these measurements. The mSWiM prediction used only OMNI data. We found that the different models provided similar solar wind predictions, as long as they used the same initial data set. The comparison of Earth-based and *STEREO-A* based predictions however shows significant deviations in the end of 2015 July, which is due to the change in the solar source sometime during its rotation from the Earth to the comet direction. Thus, we assume that the solar wind estimate from *STEREO-A* (which was actually the nearest solar wind observing spacecraft) is somewhat more reliable on those days. Unfortunately, during the investigated time period *STEREO-A* provided only sparse data due to its opposition to the Earth.

In our second method, B_0 is calculated by inverting the solution of the Cravens model, using the spacecraft's position and the B magnetic field value measured in that position as inputs. As far as the Cravens model is accurate, this method gives the exact value of B_0 and thus the solar wind dynamic pressure. This method however can only be applied outside the cavity, where $B \neq 0$, but can be used to test the accuracy of the other methods, which give estimates even if the spacecraft is inside the cavity.

The third method is based on Madanian et al. (2016b), which proposed a method to approximate the value of B_0 by searching for peaks in the *Rosetta* magnetic field data. This method only gives us an estimate, as the spacecraft probably rarely sampled the real B_0 maximum values in the pile-up region. Local peaks in the data could be caused by the spacecraft moving towards and then away from (but not necessarily reaching) the position where $B(r)$ reaches its maximum (B_0) or also by the temporal variation of the

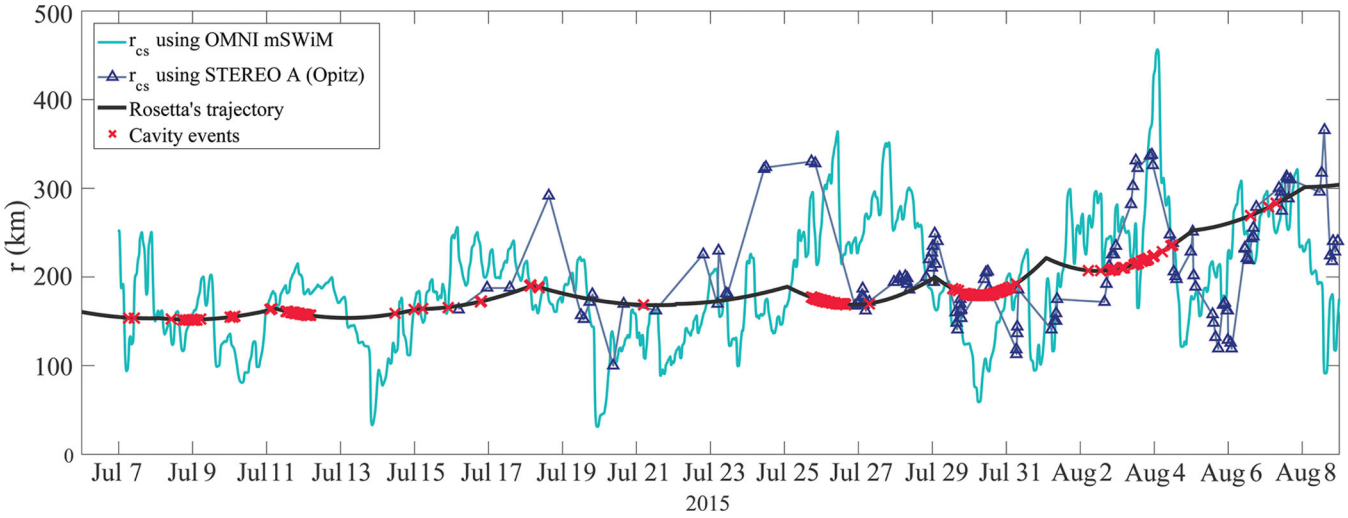

Figure 1. Cavity boundary distance calculated using solar wind pressure estimates from Earth-based mSWiM solar wind predictions (continuous blue line) and also from *STEREO-A* data propagated by simple ballistic propagation (dark blue triangles). Earth-based predictions fit the cavity observations adequately in most of July and in August, but *STEREO-A* based predictions provide a much better fit for the end of July.

magnetic field. In the former case, carefully choosing and averaging the peaks may give a good representation of B_0. We usually find cavity crossings where these B_0 values are relatively small, meaning that the diamagnetic cavity is less compressed. We used this method as well and tested its accuracy.

First, we calculated the boundary distances for the time interval between 2015 July 7 and August 8 a few weeks before the comet's perihelion, and compared the results to the locations of the cavity events found by Goetz et al. (2016b) and Nemeth et al. (2016). In this time period, the spacecraft was located 150–300 km from the nucleus, near to the comet's terminator plane. After validating the method on this time interval, we extended our studies for the 10 months between 2015 April and 2016 February, which contain all the cavity observations reported by Goetz et al. (2016a).

3 CAVITY BOUNDARY DISTANCE

The cavity boundary distance can be calculated according to equations (2) and (3), using various estimates for the solar wind dynamic pressure and for the outgassing rate. We performed several such calculations, and compared them with the cavity measurements. For a perfect model, the calculated boundary distance should be greater than (or equal to) the spacecraft's distance from the nucleus only at the locations of the cavity events, and smaller everywhere else. Uncertainty of the estimates as well as fluctuations in the input data and also problems with the model we use can lead to deviations from the perfect fit.

One method to estimate the solar wind dynamic pressure is to propagate the solar wind data measured by other spacecraft to the position of *Rosetta*. Here, we used the solar wind dynamic pressure estimates of various solar wind propagation methods using the data of *WIND*, *ACE*, OMNI and *STEREO-A*. For the global outgassing rate, we have used the data derived by Hansen et al. (2016). The cavity distances calculated according to equation (3) using solar wind pressure estimates from Earth-based mSWiM solar wind predictions (Zieger & Hansen 2008) and also from *STEREO-A* data propagated by simple ballistic propagation (Opitz et al. 2009) can be seen in Fig. 1. We only show the predictions of these two methods, because other methods propagating from the same initial data give similar results. Earth-based predictions are in adequate agreement with the cavity event locations in most of July and in August, but fit poorly around the end of July. *STEREO-A* based predictions provide a much better fit for the end of July.

A more detailed and more precise fit can be achieved by estimating the pressure from the maximum of the magnetic field in the draping region. We use two methods to estimate the solar wind pressure from magnetic field measurements. The first is based on the exact form of the solution of the Cravens (1986) model, the second is based on the peak detection method of Madanian et al. (2016b).

Equations (2) and (3) do not use the actual solution of the Cravens (1986) model, only general properties of the interaction. They describe a general relationship between r_0, p_{sw}, B_0 and Q, irrespectively of the actual form of the solution. If we also take into account the form of the solution $B(r) = B_0\sqrt{1-\frac{r_{cs}^2}{r^2}}$, we can express B_0 as a function of $B(r)$ and r, the measured magnetic field, and the position where it was measured. Thus, we get a more restrictive, but exact measure for the dynamic pressure, which allows us to eliminate the error originating from the uncertainty of the pressure estimation. Substituting this B_0 into equation (2), the boundary position will be

$$r_{cs} = \left(\frac{B(r)^2}{c^2 Q^{3/2}} + \frac{1}{r^2}\right)^{-1/2}, \tag{4}$$

if B is specified in units of nT and r is measured in km, Q in molecule s^{-1}. This expression is perfect in the sense that $r_{cs} < r$ outside the cavity, but it clearly cannot estimate the size of the cavity, when the spacecraft is inside and thus $B(r) = 0$. To gather that information, we use other estimation schemes. Between the cavity events, this method will provide an exact cavity boundary distance as far as we can trust the Cravens model and the accuracy of the production rate estimate. We used the Hansen et al. (2016) production rate estimate to generate Fig. 2, showing the dynamic variation of the size of the cavity, which can change by more than a factor of 3 in a matter of hours. Most of the variations are due to changes of the solar wind pressure (mediated by the draped magnetic field), although the slow increase of the average cavity distance is due to the increasing cometary activity.

$B(r) = 0$ can be approximated from the local magnetic field measurements of RPC-MAG, using a method suggested by

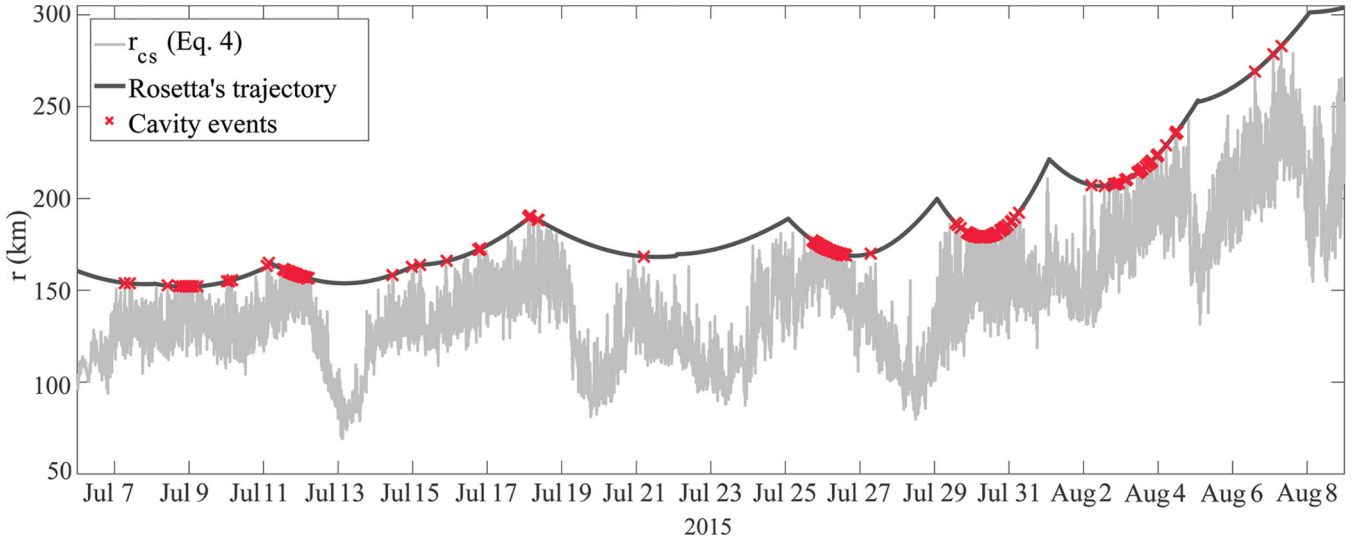

Figure 2. The boundary distance calculated from the actual measured magnetic field $B(r)$ and the position (r) of the measurement using the form of the Cravens (1986) analytical solution. This calculation can be applied only for $B(r) > 0$ (when *Rosetta* was outside the cavity).

Madanian et al. (2016b). The first step of this method is to identify well-separated significant maximum values in the *Rosetta* magnetic field data. We experimented with many different peak selection methods. Generally, the best fit to the cavity events was achieved by choosing the minimum peak prominence 10–15 nT, the minimum peak distance 5–10 min and the minimum peak value 25 nT. The latter is necessary to filter out potentially false peak values due to small amplitude field fluctuations. The elimination of these low-magnitude peaks provides a (necessary) decrease of the calculated boundary distance. Additionally, we used a smoothing filter on the magnetic field data before the peak selection to reduce high-frequency noises; we first averaged the magnetic field data by 60 s to reduce the data number before using a Savitzky–Golay filter with an order of 1 and a framelength of 5.

In Fig. 3, we demonstrate three different methods for peak selection. We choose the minimum peak prominence to be 15 nT (top and bottom panel) or 10 nT (middle panel) and the minimum peak distance 10 min. In the top panel, we used 30 s resolution *Rosetta* magnetic field data. Since we did not use a smoothing filter on the data, the result shows high-frequency fluctuations. In the other two panels, we used smoothing filters and also filtered out peak values lower than 25 nT. To precisely fit our data to the cavity events, in these two cases we used a scale factor of ∼0.9 on the calculated cavity distance. We compared these results to the boundary distance calculated by equation (4), using our first magnetic method. We can see in Fig. 3 that in the regions where $B(r) \neq 0$ the two methods give very similar boundary distance values, which means that the cavity distance calculated by the peak selection method also gives reasonable results, probably inside the diamagnetic cavity as well.

Overall, aside from a few exceptions, the results illustrated in Fig. 3 fit the observed cavity events almost perfectly. There are also some sections in the trajectory of *Rosetta*, where the calculated cavity distance is larger than the spacecraft's distance from the comet, which, according to the model, means that the spacecraft should have been inside the cavity, yet there were no cavity events found there. We carefully examined the magnetic field data in these time intervals and found many short, cavity-like signatures, which were not discovered beforehand. (A few examples are shown in Fig. 4 as green shaded areas, we also indicated the positions of these events in the middle panel of Fig. 3 by green dots.) This suggests that the Cravens neutral-drag model can accurately describe the cavity boundary distance values and it can even predict the appearance of cavity events.

We used the global outgassing rate in all the figures in the paper. Calculations using the local neutral density were also carried out, but they provided much worse fits for the measurements. Based on this observation we concluded that the local density is not sufficient to explain the size of the diamagnetic cavity. We assume that the magnetic tension suppresses the effects of local density variations, thus the cavity boundary follows the variation of the global outgassing rate. Calculations of the boundary distance using the global outgassing rate with the *Rosetta* magnetic field data are in a very good agreement with the cavity crossings, we often got one-to-one correspondence locating short cavity events, despite that in theory this method can only give an approximation for the cavity size due to the uncertainty of the selected peak values.

After validating our methods on the time period discussed above, we extended our studies to include all the cavity events observed by *Rosetta*. Fig. 5 shows our results for the time interval beginning on 2015 April 21 and ending on 2016 February 17, the red marks show cavity observations reported by Goetz et al. (2016a). The top panel features the computed cavity size using the mSWiM propagated solar wind pressure (OMNI data), the bottom panel shows the results based on *Rosetta* magnetic field measurements; the blue line is from the peak selection (or Madanian) method. The overall correspondence with the cavity observations is very good. The peak selection method works best from 2015 July to the end of that year. In 2015 June and September, the method predicts more cavity encounters than there are previously known cavity detections. Careful close examination of these periods reveals a few short cavity events, previously unknown. On the other hand, at the beginning of the cavity bearing months there are more cavity observations than that predicted by this method. As peak selection by its nature works better in larger fields this discrepancy may reflect a limitation of that method, especially since the pressure propagation method is less affected by this problem. Allowing for the temporal uncertainty of the propagation method, the quality of its prediction is fairly consistent throughout the observations, although less so before spring equinox. It is worth mentioning though that the discrepancy for both methods is most pronounced for times

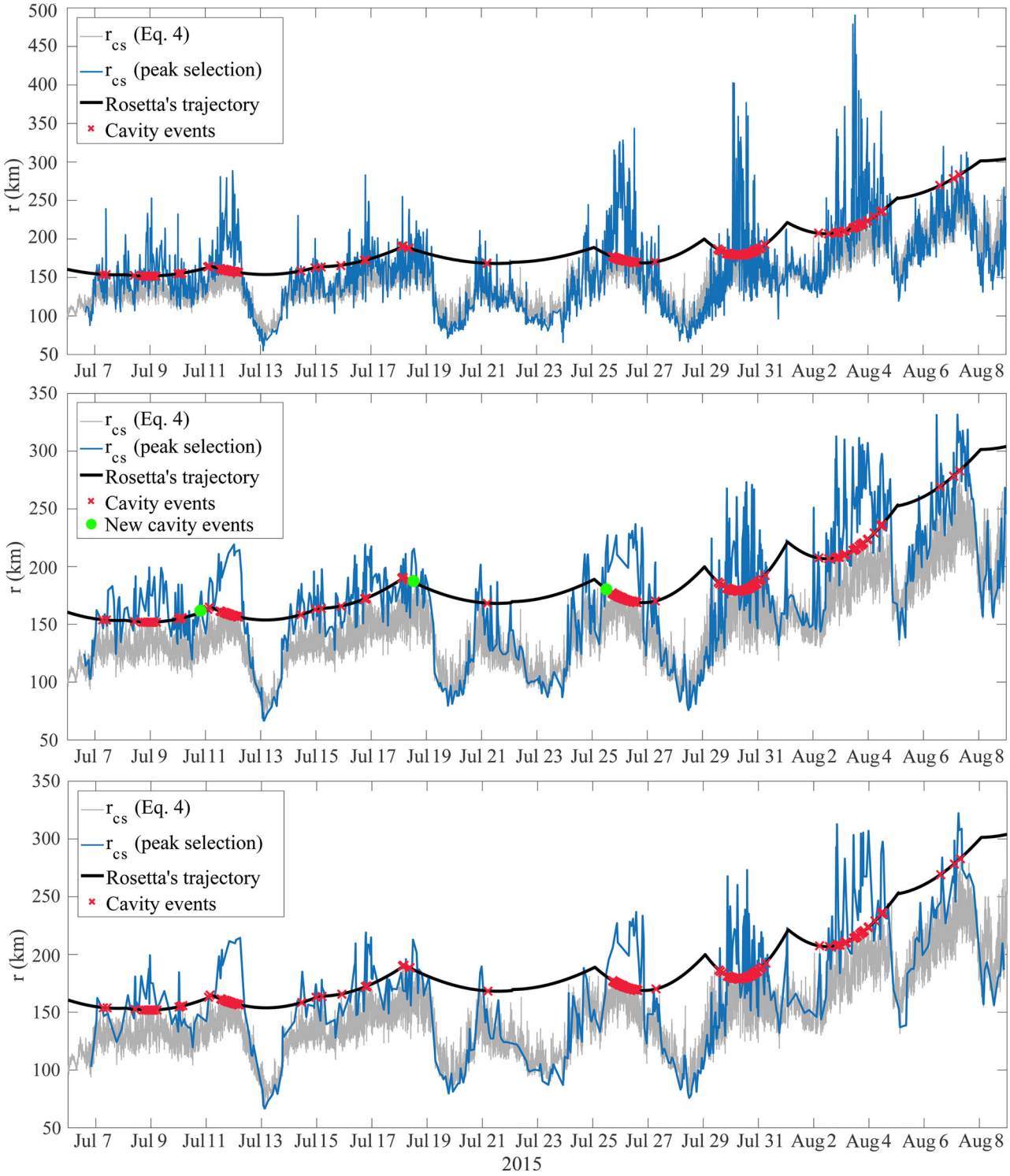

Figure 3. Cavity boundary distance calculated with different peak selection and smoothing methods (blue line) using *Rosetta* magnetic field data and global outgassing rate, compared to the boundary distance calculated by equation (4) (grey line).

before the middle of June, where Goetz et al. (2016a) found that the Q dependence of cavity event positions differs from that of later times.

Our findings suggest that the size of the cavity is indeed determined mainly by the force balance between the neutral drag and the effects of the solar wind mediated by the magnetic pressure. The slowly varying neutral production inflates the cavity, while rapid changes in the external pressure cause short-term variations. Although the predictions fit the observations well, we still cannot rule out the possibility that instabilities (as suggested by Goetz et al. 2016a,b and Henri et al. 2017) also play a role in the formation of the cavity boundary.

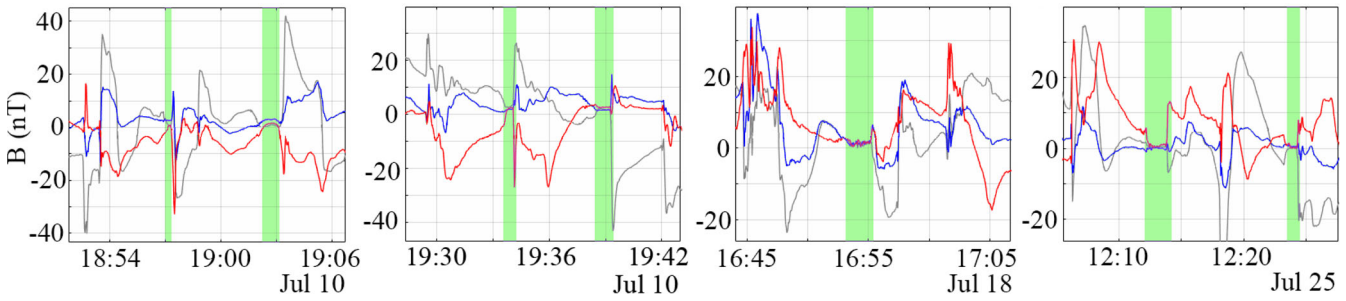

Figure 4. The predictive capability of the model. The magnetic field components are dropping to zero (highlighted with green shading) in short time intervals where the calculated boundary distance is larger than the *Rosetta*'s distance from the comet, implying short cavity like signatures that were not discovered before.

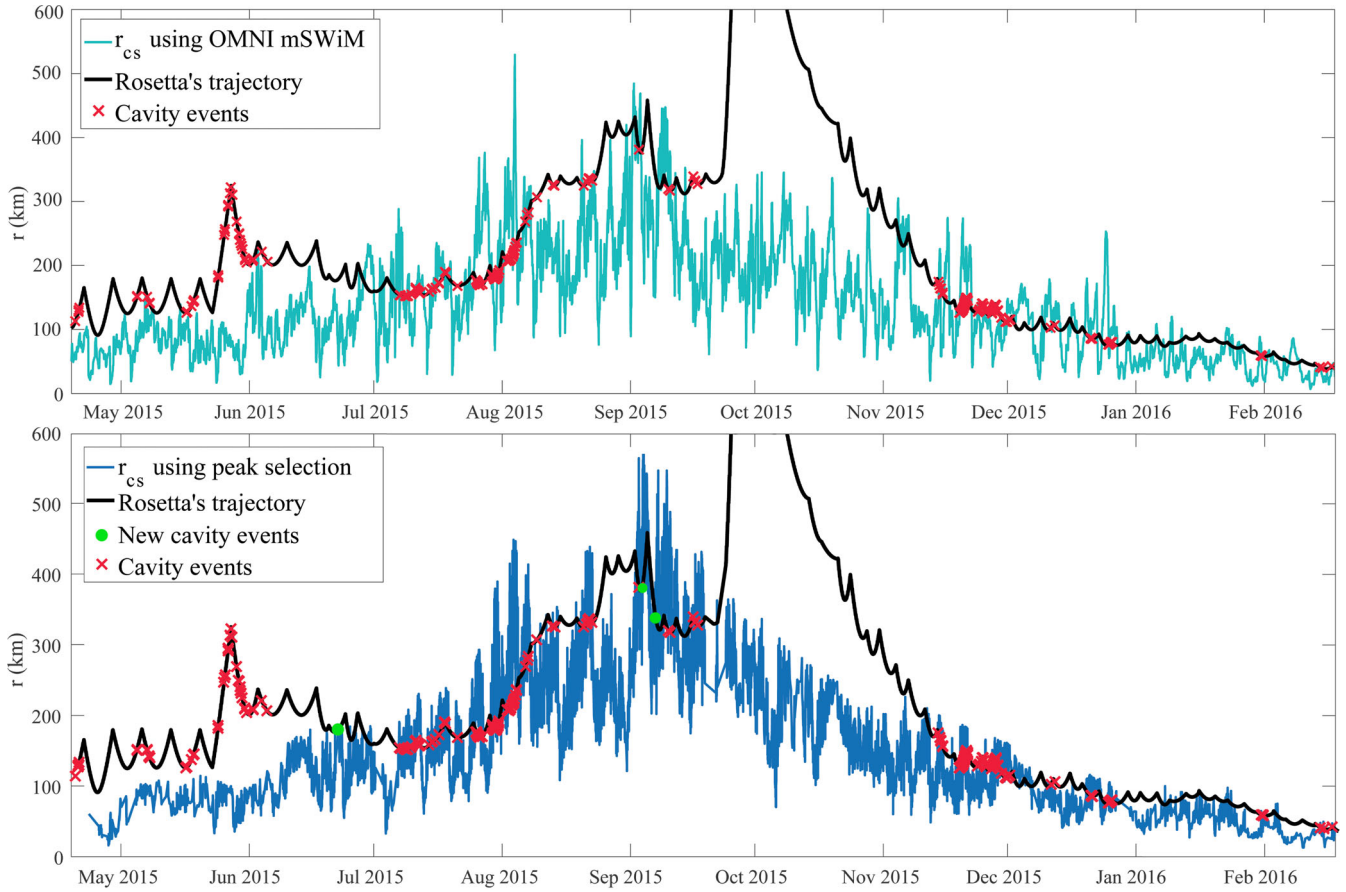

Figure 5. Cavity boundary distance calculated between 2015 April 21 and 2016 February 17 using the OMNI mSWiM solar wind dynamic pressure (top) and the peak selection method (bottom). We discovered more cavity events in the full duration data, some of these are illustrated with green dots in the bottom panel. The model fits well for the cavity events observed after mid-June, cavity events before that deviate from the model.

4 CONCLUSIONS

In this paper, we calculated the diamagnetic cavity boundary distance around comet 67P/Churyumov–Gerasimenko with various methods, using the data of *Rosetta* magnetic field and neutral density measurements and different solar wind propagation models.

We found that the boundary distance calculated with the neutral-drag model of Cravens (1986) is in a very good agreement with the observed cavity events, provided that we use accurate outgassing rate and solar wind pressure values as an input.

We calculated the boundary distance both with the local neutral density and also with the global outgassing rate, the latter providing a much better fit for the observations. This indicates that the global outgassing rate defines the position of the boundary with local pressure variations being suppressed – possibly by the magnetic tension of the field lines.

We assumed that the fast alternation of magnetized and field-free regions can be explained by the rapid changes in the external solar wind pressure at the position of the comet. We used the results of several space weather propagation methods as well as local magnetic field measurements to estimate the solar wind pressure at *Rosetta*. Propagation methods give respectable agreement with the observations. We applied two methods to estimate the pressure from the magnetic field as well. One uses the actual form of the

Cravens (1986) solution to compute the value of the field magnitude and thus the solar wind pressure. The second (Madanian et al. 2016b) uses local field maxima to approximate the parameters. Both methods give good agreement with the observations, the first providing the highest accuracy when the spacecraft is outside the cavity, but being unusable inside; the second providing good estimates for the boundary distance even when *Rosetta* dwells inside the cavity. The accuracy is so high that we were able to identify multiple previously undiscovered cavity events where the model predicted that there should be cavity crossings.

Based on these findings, we concluded that at the time of the measurements a global diamagnetic cavity existed around comet 67P, the size of which varied dynamically, closely following the changes in the cometary gas production rate and the solar wind pressure.

ACKNOWLEDGEMENTS

Rosetta is an ESA mission with contributions from its member states and NASA. We thank the *Rosetta* Mission Team, SGS and RMOC for their outstanding efforts in making this mission possible. The work was supported by the János Bolyai Research Scholarship of the Hungarian Academy of Sciences. The work on RPC-MAG was financially supported by the German Ministerium für Wirtschaft und Energie and the Deutsches Zentrum für Luft- und Raumfahrt under contract 50QP 1401. We thank K.C. Hansen and B. Zieger for providing solar wind propagations from their Michigan Solar Wind Model.

REFERENCES

Balsiger H. et al., 1986, Nature, 321, 330
Balsiger H. et al., 2007, Space Sci. Rev., 128, 745
Behar E., Nilsson H., Wieser G. S., Nemeth Z., Broiles T. W., Richter I., 2016, Geophys. Res. Lett., 43, 1411
Biermann L., Brosowski B., Schmidt H. U., 1967, Sol. Phys., 1, 254
Cravens T. E., 1986, in Battrick B., Rolfe E. J., Reinhard R., eds, ESA SP-250: ESLAB Symposium on the Exploration of Halley's Comet. ESA, Noordwijk, p. 241
Cravens T. E., 1989a, Adv. Space Res., 9, 293
Cravens T. E., 1989b, J. Geophys. Res., 94, 15025
Cravens T. E., 1991, Int. Astron. Union Colloq., 116, 1211
Dósa M., Opitz A., 2017, Geophysical Research Abstracts Vol. 19, EGU2017-14916-1, EGU General Assembly, p. 14916
Eriksson A. et al., 2016, in proc. 14th Spacecraft Charging Technology Conference. ESA/ESTEC, Noordwijk, NL
Ershkovich A. I., Flammer K. R., 1988, ApJ, 328, 967
Ershkovich A. I., Mendis D. A., 1986, ApJ, 302, 849
Galand M. et al., 2016, MNRAS, 462, S331
Galeev A. A., Cravens T. E., Gombosi T. I., 1985, ApJ, 289, 807
Gan L., Cravens T. E., 1990, J. Geophys. Res., 95, 6285
Glassmeier K.-H., Boehnhardt H., Koschny D., Kührt E., Richter I., 2007a, Space Science Reviews, 128, 1
Glassmeier K.-H. et al., 2007b, Space Sci. Rev., 128, 649
Goetz C. et al., 2016a, MNRAS, 462, 459
Goetz C. et al., 2016b, A&A, 588, A24
Goldstein B. E., Altwegg K., Balsiger H., Fuselier S. A., Ip W.-H., 1989, J. Geophys. Res., 94, 17251
Gombosi T. I., 2015, in Keiling A., Jackman C. M., Delamere P. A., eds, Physics of Cometary Magnetospheres. Wiley, New York, p. 169
Hansen K. C. et al., 2016, MNRAS, 462, 491
Henri P. et al., 2017, MNRAS, 469, S372
Huang Z. et al., 2016, J. Geophys. Res.: Space Phys., 121, 4247
Ip W.-H., Axford W., 1987, Nature, 325, 418
Koenders C., Glassmeier K.-H., Richter I., Motschmann U., Rubin M., 2013, Planet. Space Sci., 87, 85
Koenders C., Glassmeier K.-H., Richter I., Ranocha H., Motschmann U., 2015, Planet. Space Sci., 105, 101
Madanian H. et al., 2016a, J. Geophys. Res.: Space Phys., 121, 5815
Madanian H. et al., 2016b, AJ, 153, 30
Mendis D. A., Houpis H. L. F., Marconi M. L., 1985, Fundam. Cosm. Phys., 10, 380
Nemeth Z. et al., 2016, MNRAS, 462, S415
Neubauer F. M. et al., 1986, Nature, 321, 352
Nilsson H. et al., 2015a, Science. 347, aaa0571
Nilsson H. et al., 2015b, A&A, 583, A20
Odelstad E. et al., 2015, Geophys. Res. Lett., 42, 126
Opitz A. et al., 2009, Sol. Phys., 256, 365
Reinhard R., 1986, Nature, 321, 313
Rubin M., Hansen K. C., Combi M. R., Daldorff L. K. S., Gombosi T. I., Tenishev V. M., 2012, J. Geophys. Res.: Space Phys., 117, A06227
Russell C. T., Luhmann J. G., Elphic R. C., Neugebauer M., 1982, in Wilkening L. L., ed., IAU Colloq. 61: Comet Discoveries, Statistics, and Observational Selection. Univ. Arizona Press, Tucson, AZ, p. 561
Szegö K. et al., 2000, Space Sci. Rev., 94, 429
Vennerstrom S., Olsen N., Purucker M., AcuÃśa M. H., Cain J. C., 2003, Geophys. Res. Lett., 30, 1369
Vigren E., Galand M., Eriksson A. I., Edberg N. J. T., Odelstad E., Schwartz S. J., 2015, ApJ, 812, 54
Zieger B., Hansen K., 2008, J. Geophys. Res., 113, A08107

This paper has been typeset from a Microsoft Word file prepared by the author.